CHAPTER 7

Discussion and Conclusion

7.1 Discussion

In this independent study, an important gas field in offshore Vietnam have been interpreted and analyzed for hydrocarbons exploration and appraisal using both seismic dataset and one well data. The methods are applied for these purposes are 3D seismic interpretation, well log analysis and interpretation, AVO modeling and elastic impedance inversion. This chapter is focused on reviewing and discussing the works and the results that are completed in this study.

Three – dimensional seismic data is interpreted in order to understand the structural development of study area and identify forms of the potential reservoirs at and around the well location. In addition, the horizons are also used as a guideline to create the initial model in inversion process. In the interpretation process, seven horizons were picked following the formation tops in the Well A after well to seismic tie process (time - depth of the well were determined) except seabed and T10 which represents the top of Oligocene was picked following the geological report provided by the company. Seven horizons picked are shown in Figure 4.1. To guide picking horizons, the faults have to be interpreted together. In order to improve the visualization of the faults in study area, Variance seismic attribute is used to support mapping the faults (Figures 4.15 to 4.17). The Variance attribute maps are useful especially in locations where the fault planes are almost horizontal. Based on the interpreted horizons and faults, seven time structure maps are built (Figures 4.24 to 4.30). The time structure maps represent the images of the subsurface in time domain, top of two main reservoirs in Well A are shown in Figure 4.26 and Figure 4.28. To highlight the distribution of high amplitude that indicates the potential reservoir areas, RMS amplitude attribute is extracted from the seismic data, the RMS amplitude is extracted for each angle stack along two horizons

Top UMA15 and Top MMF30 (Figures 4.18 to 4.23). As expected, the variations in amplitude are clearly seen in RMS amplitude maps from near to far angle stack. It is obvious that high amplitude is at the Well A location in the far angle stack RMS map in comparison with near and mid angle stacks especially for MMF30 reservoir. The high amplitude in the far angle stack RMS map represents distribution of sand bodies in the study area.

In the Well A, there are two main dominated sandstone reservoirs: UMA15 in upper Miocene formation and MMF30 in middle Miocene formation, with the thicknesses are about 15 m and 33 m respectively. Two reservoirs could not be identified by seismic data because of the thicknesses of two reservoirs are both below the tuning thickness of the seismic data in zone of interest which are 28 m and 35 m respectively. In the logs data, the UMA15 sandstone shows low density of around 2.2 g/cc, slightly high in P-wave velocity (2850 m/s to 3150 m/s) and high S-wave velocity of around 1500 m/s to 1700 m/s compared to the surrounding shale. Meanwhile the MMF30 sandstone shows relative low density of about 2.45 g/cc, high P-wave velocity from 3700 m/s at sand intervals and 4300 m/s to 4500 m/s at interbedded shale intervals and very high S-wave velocity (around 2300 m/s) than the surrounding shale (around 1700 m/s). For other available logs data at the Well A, both two reservoirs show very high resistivity values of 10 to 15 Ohmm for UMA15 and 4 to 11 Ohmm for MMF30 at reservoir intervals that indicates presence of hydrocarbons in the reservoirs; the cross-overs between neutron porosity log and density porosity log at the two reservoirs intervals also indicates hydrocarbons in the reservoirs. The acoustic impedance (AI) log is generated at zero offset however the reservoirs could not be identifying using AI due to very small or no difference in AI value between the reservoirs interval with the above and under intervals. Therefore, three elastic impedance logs are calculated at 6.5 degrees, 19.5 degrees and 33 degrees for near, mid and far angle stacks (Figure 6.1) using equations from Connolly, 1999. The near (0 – 13 degrees), mid (13 – 26 degrees) and far (26 -40 degrees) angle stacks are also generated depending on the RMS velocity model provided by the company.

The AVO gradient analysis process is carried out in order to test AVO attribute parameters for each reservoir. By calculating amplitude using two terms Aki – Richards

approximation and plotting amplitude in intercept and gradient plot, the AVO class 2 for UMA 15 reservoir an AVO class 2P for MMF30 reservoir are defined by analyzing amplitude variations with angle for top and base of the reservoirs. The key to using AVO for fluid identification is comparison of real seismic data with a synthetic seismogram (Chiburis et al., 1993). Thus, AVO synthetic models are constructed for both two reservoirs UMA15 and MMF30 (Figures 5.19 to 5.22). The fluid replacement modeling is main part of AVO modeling process, it allows testing the variations of AVO models with different fluids conditional scenarios. Three fluids scenarios are tested involving 100% water saturation, 100% gas saturation and brine and gas saturation variations. Finally, the presences of gas in both two interest reservoirs are proved be comparing synthetic models with the actual seismic full angle gather.

By cross plotting the elastic impedance parameters of near, mid and far logs against each other for each reservoir intervals (Figures 5.5 to 5.10), AVO anomalies zones are highlighted due to the different trend between AVO in the reservoirs and AVO outside reservoirs.

Elastic impedance inversion is carried out to extract rock properties from seismic data. The impedance inversion process is applied for each angle stack to generate inverted seismic volumes. The wavelets used in inversion process are wavelets extracted after well to seismic tie process for each angle stack. Amplitude and phase spectrum of these wavelets are estimated using rotating zero phase synthetic method. Before inversion process, the low frequencies initial models are created for near, mid and far angle stacks (Figures 6.11 to 6.13). The input initial strata models of the inversion process are low frequencies models after a low pass filter were applied. Three inverted elastic impedance volumes are generated at 6.5 degrees (inverted EI_near), 19.5 degrees (inverted EI_mid) and 33 degrees (inverted EI_far) after inversion processes (Figures 6.14 to 6.19). It obvious that two sandstone reservoir at around 2515 ms and 2920 ms are easier identified with surrounding shale in the far inverted volume in comparison with the near and mid inverted volume due to the low elastic impedance value. The distributions of potential hydrocarbon zones which have AVO anomalies are highlighted in the seismic section when cross plotting EI_near and EI_far. The AVO anomalies zones identified from log data is used to highlight data in seismic. By using

elastic impedance inversion the upper Miocene UMA15 gas bearing sandstone reservoir which has class 2 AVO is more convincing. Meanwhile elastic impedance inversion is really useful for 2P AVO class as the middle Miocene MMF30 gas bearing sandstone reservoir which cannot be identified by convention acoustic impedance inversion.

Lithology in zone of interest (2900 m to 3800 m) of the well A could be differentiate by the cross plot of AI versus EI_far for the Well A as shown in Figure 7.1. Logs data is plotted by Gamma Ray values. It is clearly that the cleanest sand reservoir sands can have the same acoustic impedance (AI) range as some shales , for example around 7500 (m/s)*(g/cc) in horizontal axis. However, the same sands on EI_far axis have noticeably lower value than the corresponding shales. This means that sands cannot be distinguished from shales using only acoustic impedance , but if one uses both AI and EI simultaneously it can design a cut-off trend line that can help distinguish sands from shales (Savic et al., 2000).

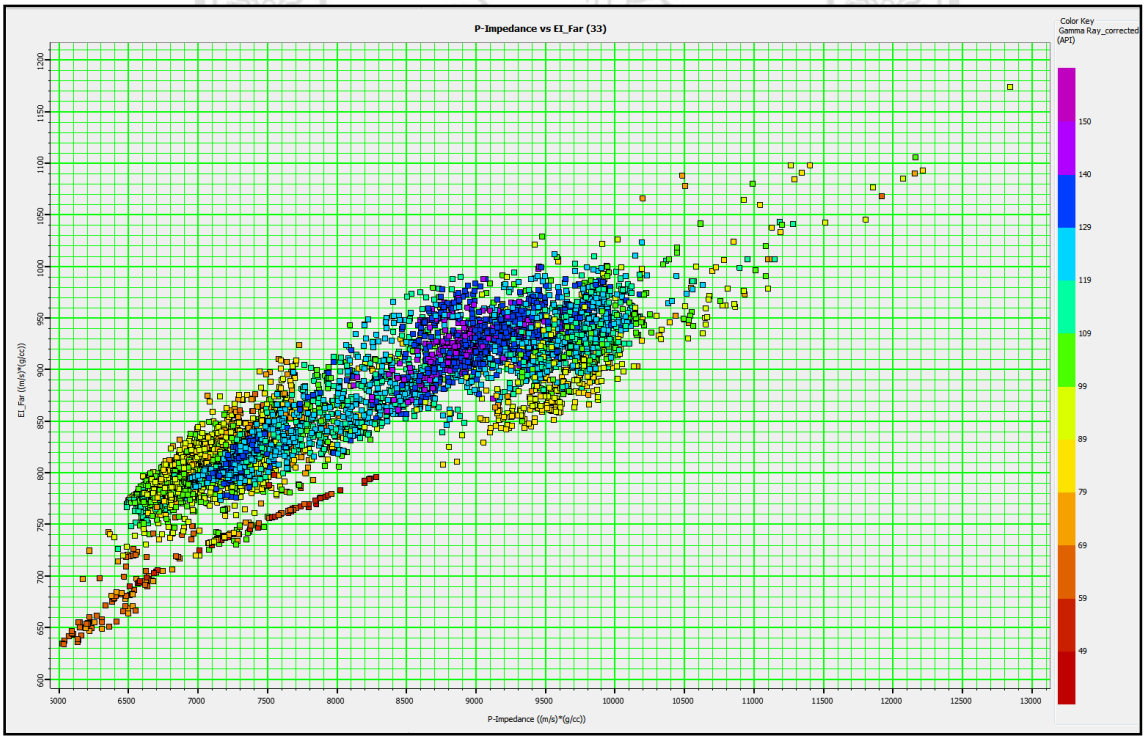

Figure 7.1: Cross plot of AI versus EI_far for the Well A.

Figures 7.2 to 7.4 show the elastic impedance (EI) maps through Top UMA15 of inverted near, mid and far angle stack volumes accordingly. The EI maps are generated along the horizon Top UMA15 with time window of 30 ms under the horizon. It is

obviously that elastic impedance parameters vary between inverted near, mid and far angle stack volume. Elastic impedance shows lowest value from around 762 to 780 (m/s)*(g/cc) in the inverted far angle stack volume that indicates distribution zones of gas saturated sand. There is a zone in the South of the study area which has low elastic impedance around 762 to 770 (m/s)*(g/cc) from inverted near to far angle stack volumes, that zone can be a potential reservoir. In the West and North West of study area, there is a big area where elastic impedance is relative low to low in the inverted near angle stack volume, however in the inverted far angle stack volume, that location show relative high elastic impedance. This means that location is not the hydrocarbon bearing zone.

Figures 7.5 to 7.7 show the elastic impedance maps through Top MMF30 of inverted near, mid and far angle stack volumes respectively. The EI maps are generated along the horizon Top UMA15 with time window of 30 ms under the horizon. It is clearly that elastic impedance parameters vary between inverted near, mid and far angle stack volume. The MMF30 gas bearing sandstone reservoir zone could be identified only in the inverted far angle stack volume due to very low inverted EI_far value of around 880 to 895 (m/s)*(g/cc). The reservoir (black dashed zone) is located in the flank between a main fault and a synthetic fault. In the hanging wall of the synthetic fault, there is a smaller area that also shows low EI in inverted far angle stack volume, that area can be a potential hydrocarbon reservoir. In the West and North West of study area, there is a big area where elastic impedance is relative low to low in the inverted near and mid angle stack volume. However, this area show higher elastic impedance in the inverted far angle stack volume, so this area is not good place for hydrocarbon exploration.

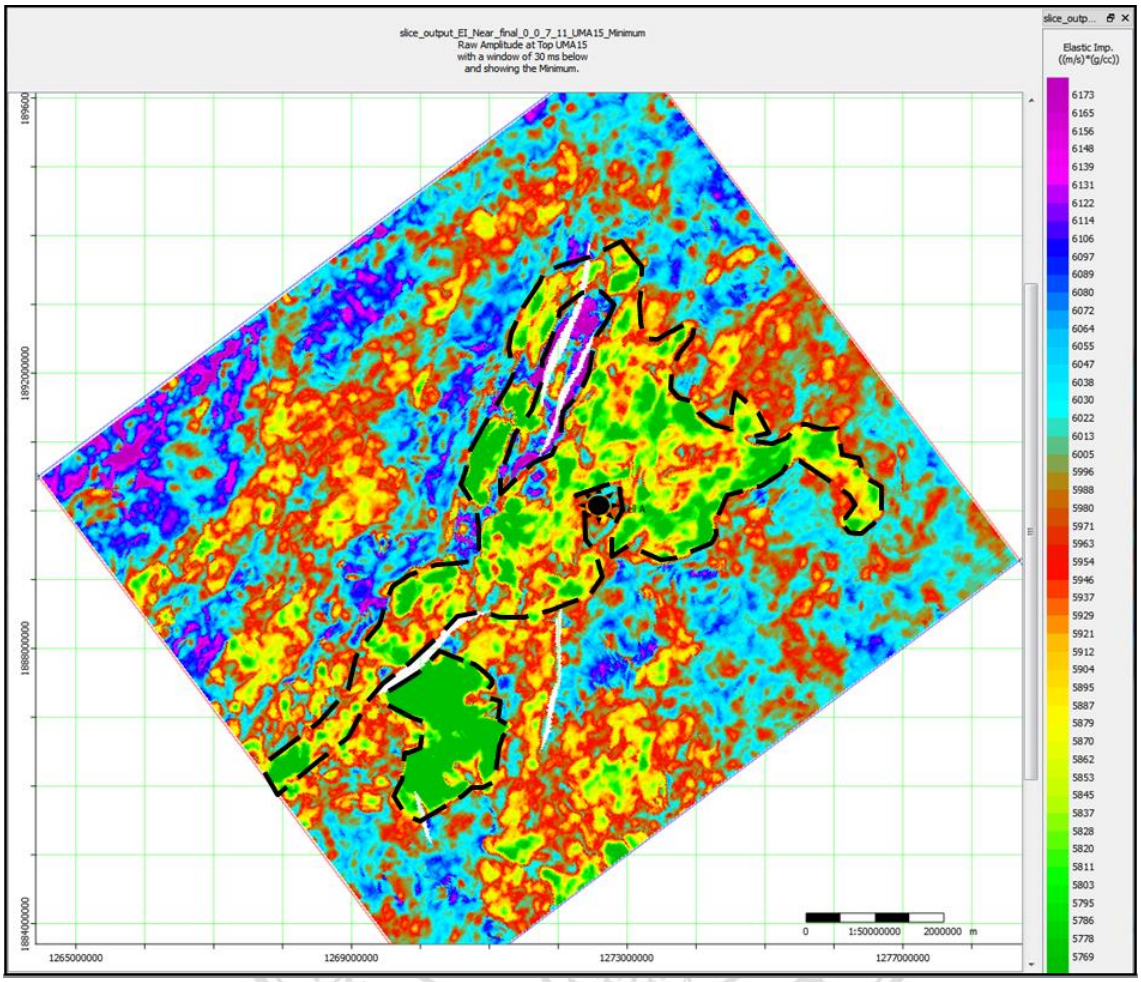

Figure 7.2: Elastic impedance map through horizon Top UMA15 of inverted near angle stack volume. The black dashed lines represent low elastic impedance zones.

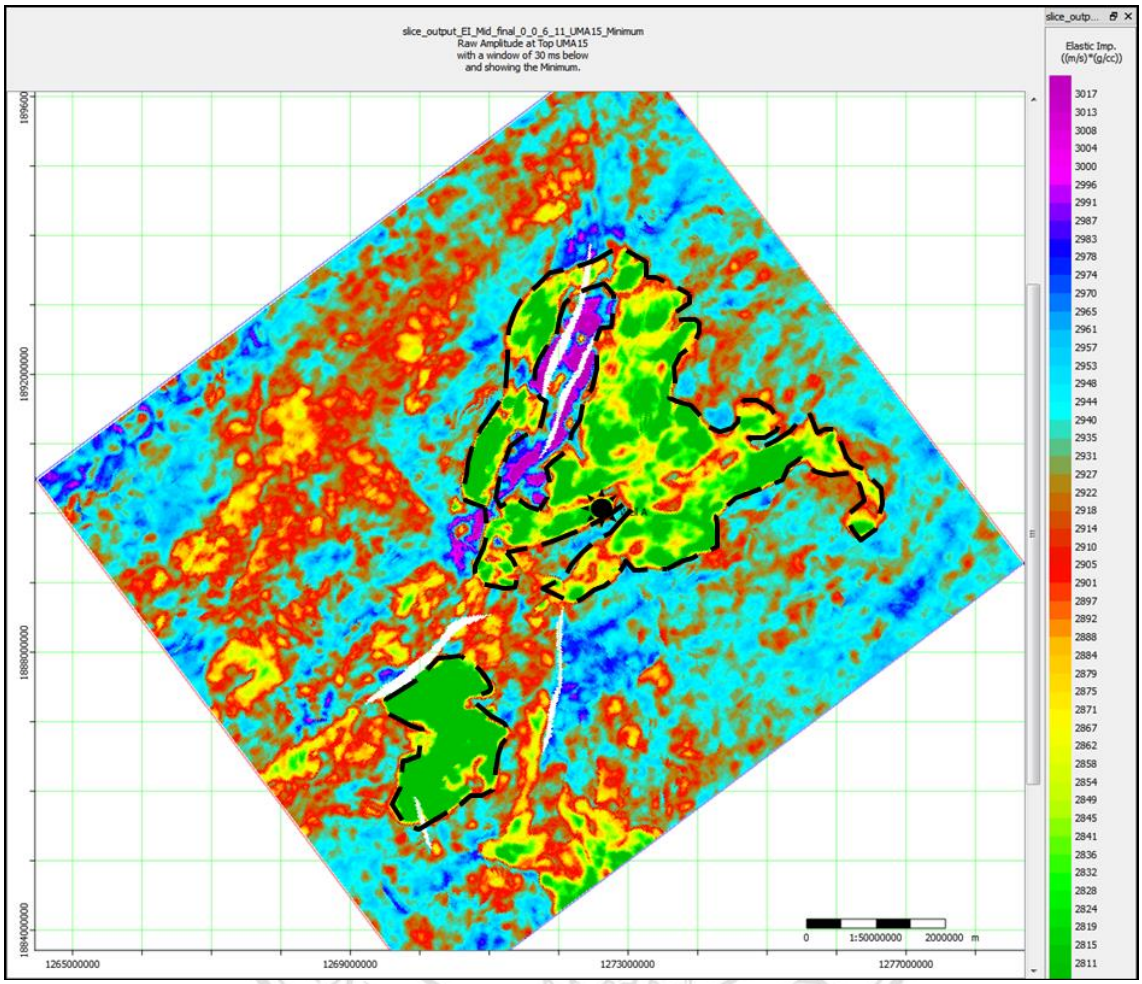

Figure 7.3: Elastic impedance map through horizon Top UMA15 of inverted mid angle stack volume. The black dashed lines represent low elastic impedance zones.

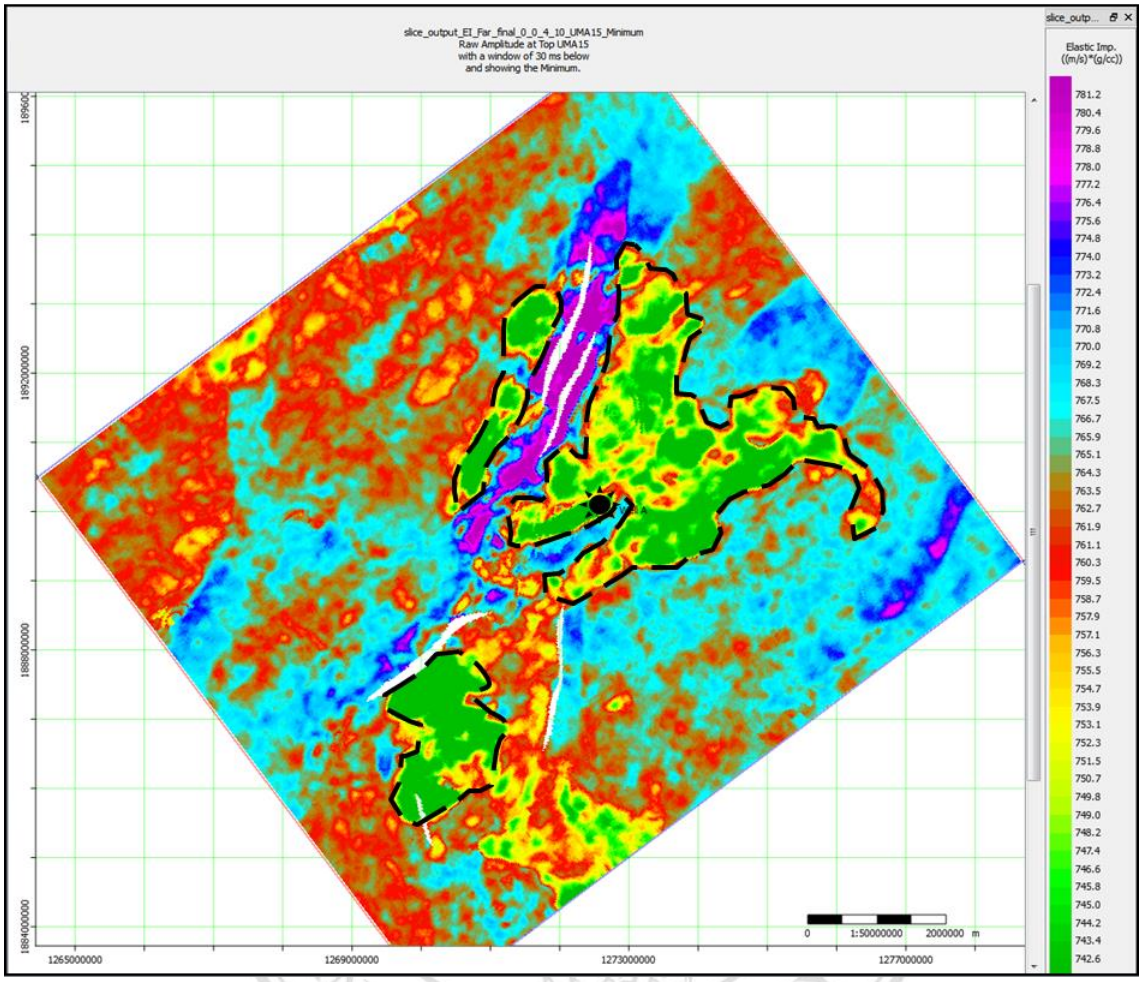

Figure 7.4: Elastic impedance map through horizon Top UMA15 of inverted far angle stack volume. The black dashed lines represent low elastic impedance zones.

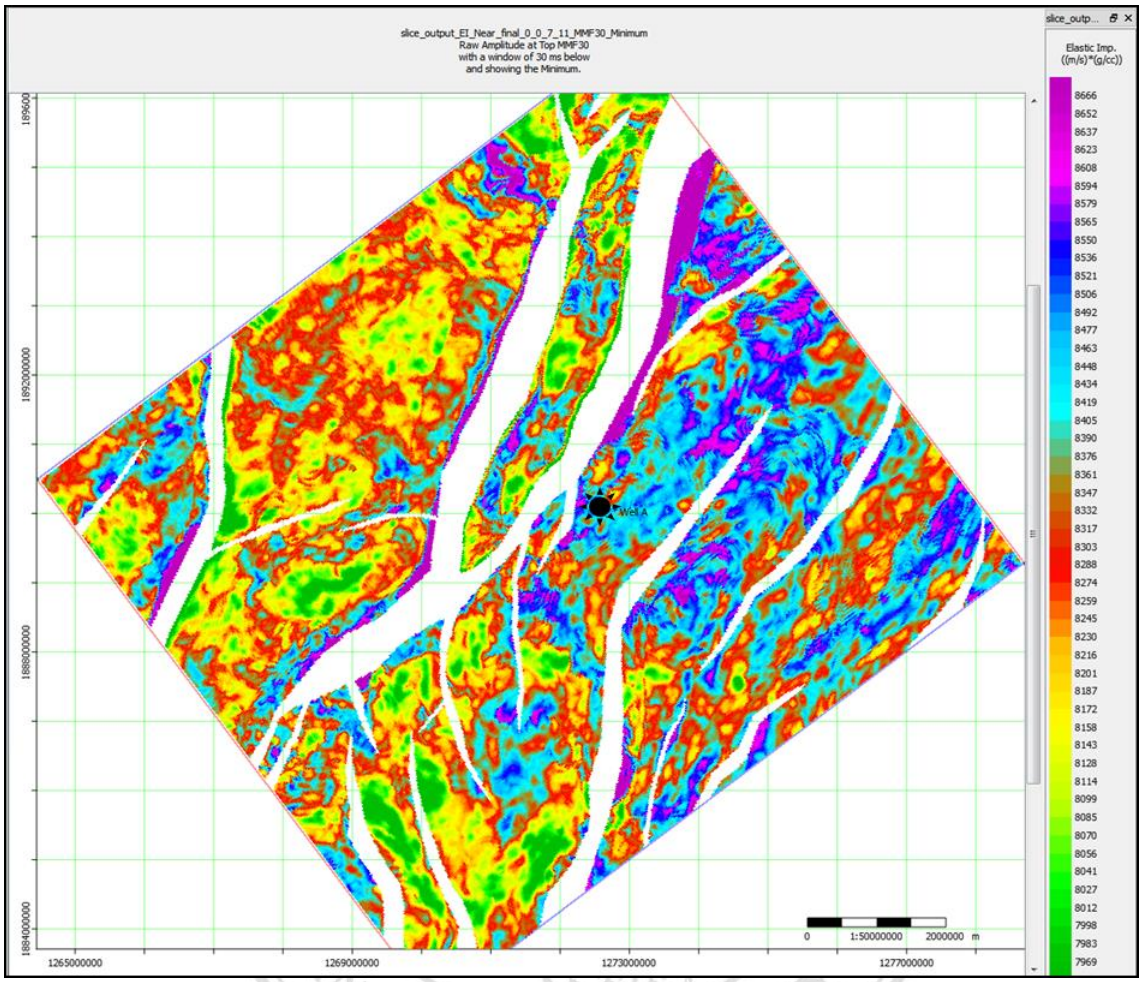

Figure 7.5: Elastic impedance map through horizon Top MMF30 of inverted near angle stack volume.

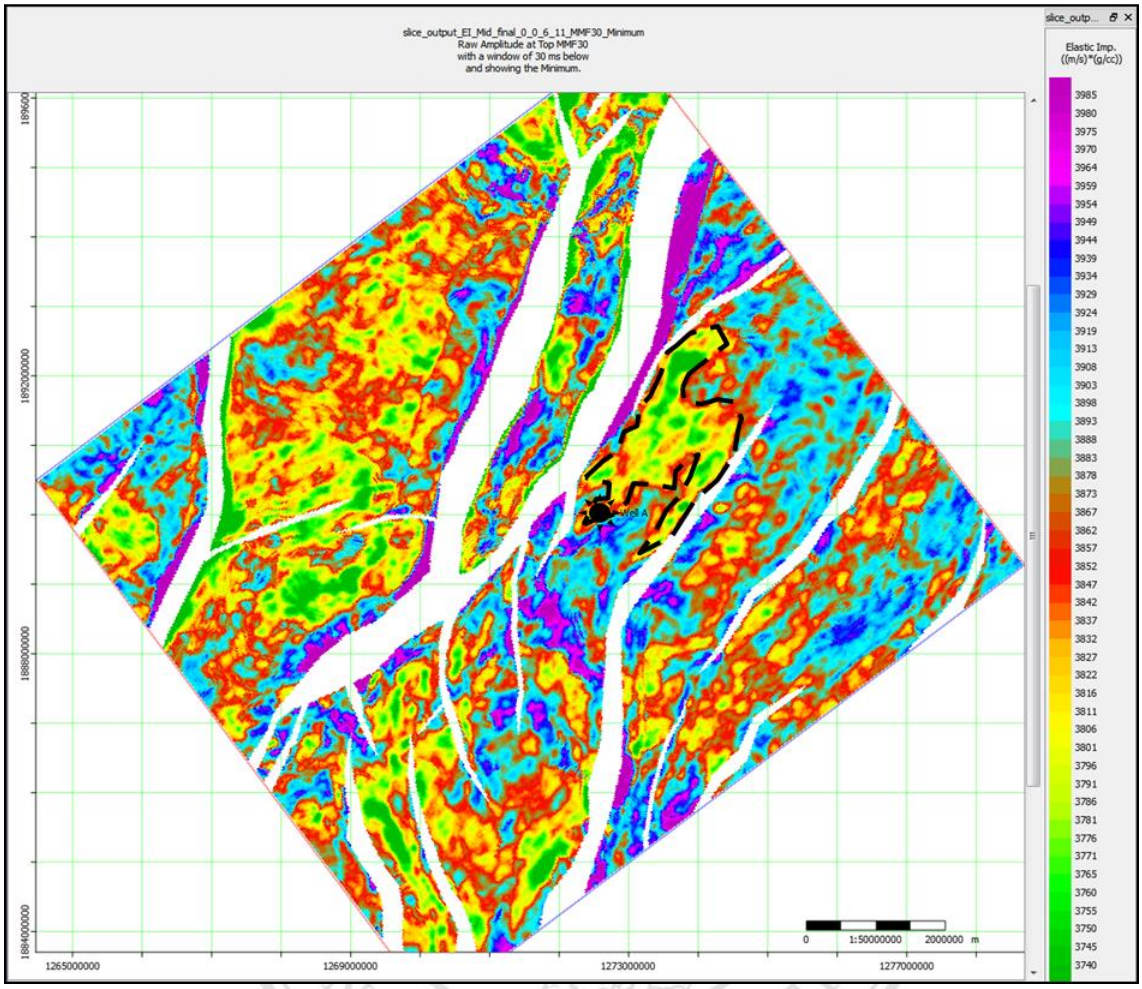

Figure 7.6: Elastic impedance map through horizon Top MMF30 of inverted mid angle stack volume. The black dashed line represents low elastic impedance zone.

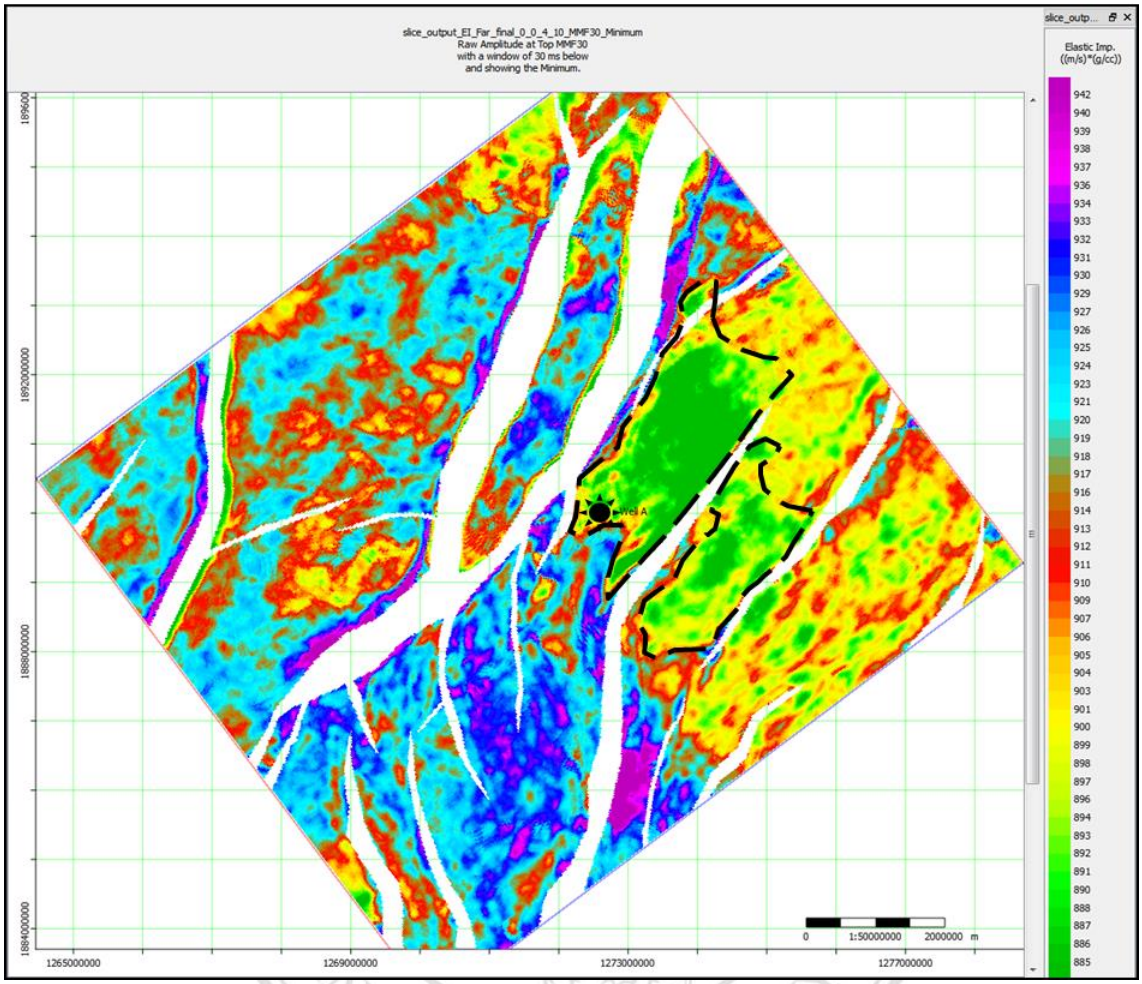

Figure 7.7: Elastic impedance map through horizon Top MMF30 of inverted far angle stack volume. The black dashed line represents low elastic impedance zone.

7.2 Conclusion

Quality control and generation of logs data are very important for any inversion process because bad logs data can affect negatively to the inversion results. Besides, integration of petrophysics and rock physics by cross plotting elastic parameters such as Vp, Vs and density provides understanding about the physical properties of the rock in the well location. This information is helpful for delineating the lithology and fluids types.

The fluid types in the reservoirs could be delineated easier by constructing AVO synthetics for various expected fluid scenarios and comparing the corresponding synthetic seismograms with the actual seismic data.

Elastic impedance inversion promotes its efficiency in comparison with acoustic impedance in identification gas bearing sand reservoirs especially for class 2 and class 2P AVO response. This because of elastic impedance inversion method is applied for pre-stack dataset which could involve AVO effects into analysis seismic reflectivity. Besides, elastic impedance gives more convincing images of the potential reservoir than which acoustic impedance does.

Difference in AVO classes between two main reservoirs in the Well A causes difference in impedance inversion results for two reservoirs. For class 2 AVO of the reservoir, elastic impedance result shows clearly the interest zone even in near angle stack. Nevertheless, for class 2P AVO of the reservoir, elastic impedance result shows clearly the zone of interest in only far angle stack. The main reason for that is amplitude of reflectivity of class 2P AVO is near the zero amplitude.